Simulation and analysis of the aeroelastic-galloping-based piezoelectric energy harvester utilizing FEM and CFD

Ismoyo Haryanto[1,*], *Achmad* Widodo[1] , *Toni* Prahasto[1], *Djoeli* Satrijo[1], *Iswan* Pradiptya[2], and *Hassen* Ouakad[2]

[1]Mechanical Engineering Department, Faculty of Engineering, University of Diponegoro, Tembalang, Semarang, Indonesia

[2]Mechanical Engineering Department, College of Engineering Sciences and Applied Engineering King Fahd University of Petroleum & Minerals, Dhahran, 31261, Kingdom of Saudi Arabia

Abstract. Due to a large oscillation amplitude, galloping can be an admissible scenario to actuate the piezoelectric-based energy harvester. In the case of harvesting energy from galloping vibrations, a prismatic bluff body is attached on the free end of a piezoelectric cantilever beam and the oscillation occurs in a plane normal to the incoming flow. The electrical power then can be extracted from the piezoelectric sheet bonded in the cantilever structure due to the dynamic strain. This study is proposed to develop a theoretical model of a galloping-based piezoelectric energy harvester. A FEM procedure is utilized to determine dynamic characteristics of the structure. Whereas the aerodynamic lift and drag coefficients of the tip bluff body are determined using CDF. The results show that the present method gives precise results of the power generated by harvester. It was found that *D*-section yields the greatest galloping behavior and hence the maximum power.

1 Introduction

The lifespan limitation of small batteries is one of the main challenges in the standalone systems/self-power devices application such as a wireless sensor network [1]. Structural vibration is one of the most used mechanical domain which enables to be converted into electrical field by utilizing several well-known energy harvester. Piezoelectric-based vibration energy harvester has been used as favorable transduction mechanism by many researchers due to its simplicity, efficient and wide range operational frequencies. There are many studies have been published aiming the investigation of piezoelectric energy harvester as an electronic devices power supply, either as redundant charging system or primary power supply [2,3,4,5]. There are increasing research interest of aeroelastic-based energy harvesters including vortex-induced-based and galloping-based energy harvesters. Galloping is one of the classical aeroelastic instabilities phenomena which can be

* Corresponding author: ismoyo_h@undip.ac.id

characterized as a low-frequency and large-amplitude oscillation. As an aeroelastic phenomenon, galloping is generated by a coupling between the forces of aerodynamic, elastic and inertia. Because causing a large oscillation amplitude, galloping can be an admissible scenario to actuate the piezoelectric-based energy harvester. In the case of harvesting energy from galloping vibrations, a prismatic bluff body is attached on the free end of a piezoelectric cantilever beam and the oscillation occurs in a plane normal to the incoming flow. The electrical power then can be extracted from the piezoelectric sheet which bonded in the cantilever structure due to the dynamic strain.

2 Analytical modeling of energy harvester

Figure 1 shows a prismatic bluff body tip mass having a *D*-, square, or triangular -section is mounted at the tip of a flexible cantilever beam. When the bluff body is facing an incoming wind flow, then the occurring of wind-induced vibration causes the box to gallop in the transverse direction, leading to self-excited bending vibrations in the beam. Energy is harvested due to the motion of the piezoelectric sheet bonded in the cantilever beam, whose terminals are connected across a load resistance.

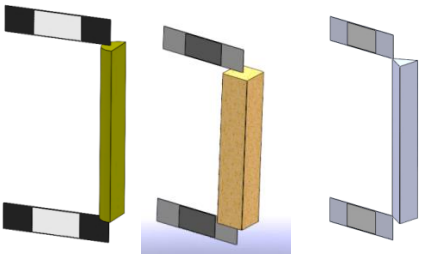

(a) (b) (c)

Fig. 1. A schematic illustration of energy harvester with tip body having section of (a) *D*, (b) square and (c) triangular.

2.1 Aerodynamic model

Figure 2 shows a section which is exposed to an air flow with a mean speed U and undergoing both transverse and angular displacements denoted by w and θ, respectively. The generated lift (L) and drag (D) forces are then formulated as

$$L = \tfrac{1}{2}\rho(U^2 + (\dot{w}(L_b))^2)b_{tip}C_L \tag{1}$$

$$D = \tfrac{1}{2}\rho(U^2 + (\dot{w}(L_b))^2)b_{tip}C_D \tag{2}$$

where ρ is the air density , b_{tip} is the bluff body section width, $\dot{w}$ is the transversal velocity, and C_L and C_D are the lift and drag coefficient, respectively. The aerodynamic analysis is conducted for determining C_L and C_D with the effective angle of attack of α. On the tip body the effective angle of attack is given by

$$\alpha = \tan^{-1}\left(\dot{w}(L_b)/U\right) + w'(L_b) \tag{3}$$

Projection of the lift and drag components along the vertical direction gives the excitation force F_{tip} in the downward as

$$F_{tip} = F_z L_{tip} = \left(L\cos\alpha + D\sin\alpha\right)L_{tip} = ½\,\rho U_{rel}^2 L_{tip} C_y \tag{4}$$

where $U_{rel} = \sqrt{U^2 + \left(\dot{w}(L_b)\right)^2}$, $C_y = C_L\cos\alpha + C_D\sin\alpha$ and L_{tip} is length of bluff body.

Assuming small values of the velocity ratio $\dot{w}/U$, the force coefficient can be expanded in powers of the angle of attack as follows

$$C_y(\alpha) = \sum_{j=0}^{n} a_j \alpha^j = \sum_{j=0}^{n} a_j \left(\frac{\dot{w}}{U}\right)^j \tag{5}$$

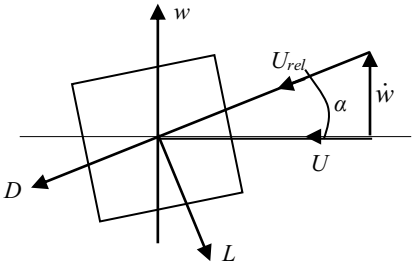

Fig. 2. Aerodynamic loads acting on the section of bluff body.

2.2 Structural Analysis

Consider a cantilever beam bonded with piezoelectric sheets. Both of the beam and the piezoelectric sheets are considered as Euler-Bernoulli Beam elements. So the elemental stiffness matrix [*k*] and mass matrix [*m*] of beam element are

$$[k] = \frac{EI}{l_p^3}\begin{bmatrix} 12 & 6l_p & -12 & 6l_p \\ 6l_p & 4l_p^2 & -6l_p & 2l_p^2 \\ -12 & -6l_p & 12 & -6l_p \\ 6l_p & 2l_p^2 & -6l_p & 4l_p^2 \end{bmatrix} \quad ; \quad [m] = \frac{\rho A l_p}{420}\begin{bmatrix} 156 & 22l_p & 54 & -13l_p \\ 22l_p & 4l_p^2 & 13l_p & -3l_p^2 \\ 54 & 13l_p & 156 & -22l_p \\ -13l_p & -3l_p^2 & -22l_p & 4l_p^2 \end{bmatrix} \tag{6}$$

In which $EI = E_bI_b + 2E_pI_p$ is the flexural rigidity and $\rho A = b_b(\rho_b t_b + 2\rho_p t_p)$ is the mass per unit length of a bonded Beam-Piezoelectric Element. In the present study suffix '*b*' is used for regular beam element, suffix '*p*' is used for piezoelectric element. If *w* indicates the vertical displacements of the beam, $[\overline{M}]$ and $[\overline{K}]$ are global mass and stiffness matrices of the structure, respectively, then the equation of motion for free vibration of entire structure is

$$[\overline{M}]\{\ddot{w}\} + [\overline{K}]\{w\} = 0 \tag{7}$$

Solving Equation (7) gives natural frequencies, ω_n, and mode shapes, ϕ, of the system.

2.3 Equation of motion

The coupled matrix differential equations for a piezoelectric energy harvester, namely electromechanic equation, can be formulated with respect to the generalized coordinate *u* and the voltage generated by the piezoelectric sheets *V* as

$$M\ddot{u} + Ku + \Theta V = F_{tip}\phi(L_b) \tag{8}$$

$$\Theta^T u + \frac{1}{C_P} V + R_L \dot{V} = 0 \tag{9}$$

where M and K are matrices of generalized mass and generalized stiffness of the system, respectively. Whereas Θ is the electromechanical coupling coefficient defined as $\Theta = -E_p\ d_{31}\ b_p\ (t_p + t_b)/2$, where d_{31} is strain coefficient of the piezoelectric. In Equation (9) $C_P = e_{33} A_p / t_p$ is the capacitance of the piezoelectric sheets (at constant strain), where e_{33} is dielectric constant of the piezoelectric. By defining a state vector containing the generalized displacement, generalized velocity, and charge, $X = [X_1 \quad X_2 \quad X_3]^T = [u \quad \dot{u} \quad q]^T$ the equations of motion (Equations (8) and (9)) can be rewritten as

$$\begin{aligned} \dot{X}_1 &= X_2 \\ \dot{X}_2 &= -\left(M^{-1}K\right)X_1 - \left(M^{-1}\Theta\right)X_3 - (M^{-1}\phi(L_P))F_{tip} \\ \dot{X}_3 &= -\left(\frac{1}{R_L}\Theta^T\right)X_1 - \left(\frac{1}{R_L C_P}\right)X_3 \end{aligned} \tag{10}$$

Equation (10) can be solved using standard numerical method to obtain time response of displacement, velocity and electrical charge of harvester.

3 Results

Table 1 shows the geometrical and material properties of cantilever beam and piezoelectric which are applied in this study. A tip mass of 0.08 kg was used for generating galloping. The CFD analysis was performed to obtain the variation of lift and drag coefficients (C_L and C_D) at angles of attack ranging from -45º to 45º and at Reynolds number of 10800.

Table 1. Geometrical and material properties harvester.

Parameter	Cantilever Beam	Piezoelectric
Material	Aluminium	Piezoelectric PZT-5H
Length (m)	$l_b = 0.161$	$l_p = 0.0724$
Width (m)	$b_b = 0.038$	$b_p = 0.0362$
Thickness (m)	$t_b = 0.00635$	$t_p = 0.267 \times 10^{-3}$
Young's modulus (N/m^2)	$E_b = 6.9 \times 10^{10}$	$E_p = 6.2 \times 10^{10}$
Density (kg/m^3)	$\rho_b = 2700$	$\rho_p = 7800$
Damping Constants	$\alpha = 0.001$, $\beta = 0.0001$	-
Stress Constant (Vm/N)	-	$g_{31} = 8.5 \times 10^{-3}$
Strain Constant (C/N)	-	$d_{31} = -320 \times 10^{-12}$
Dielectric Constant (nF/m)	-	$e_{33} = 33.65$

The natural frequency of the present energy harvester was found to be 21.90 Hz. Figure 3 shows a comparison of measured and predicted output voltage when air speed 4.47 m/s and load resistance 37 kΩ for a triangular cross section. It can be seen that the trend of the predicted voltage closely approximates that of the measured voltage and the steady-state behavior correlates very well with predictions. Furthermore, this method is applied to predict the characteristic of energy harvester with bluff body of *D*- and rectangular section.

Figures 4a and 5a show samples of the velocity field distribution for Reynolds number of 10800 obtained using CFD to determine C_L and C_D for *D*- and rectangular section, respectively. Having been C_L and C_D determined the aerodynamic coefficient C_Y can be calculated. The approximation of C_Y then can be conducted utilizing Equation (4). Table 2 shows the constant coefficients for approximate C_Y for *D*- and square section. Meanwhile, the comparison of calculated and approximated of C_Y are shown by Figure

4b and 5b. Figure 6 and 7 show the real part of first eigenvalue and the time history of the output voltage plots for the *D*- and square section for a load resistance of 37 kΩ and an air speed of 4.47 m/s. It can be noted that the galloping onset for *D*- and square section are 1.85 m/s and 3.05 m/s, respectively.

Table 2. Constant coefficient of polynomial for C_y approximation

Section	a_0	a_1	a_2	a_3	a_4	a_5	a_6	a_7	a_8	a_9
D-section	0	0.57	-0.05	0.82	0.41	-24.0	-1.00	83.3	0.76	-73.5
Square	0	1.70	0	-21.0	0	48.0	0	-35.0	-	-

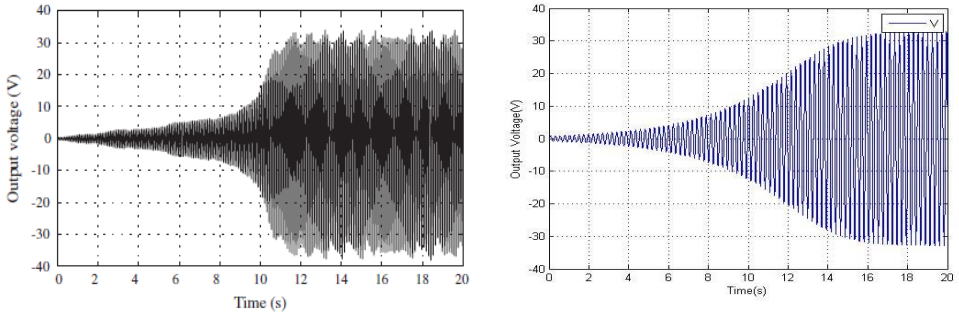

(a) (b)

Fig. 3. (a) Measured output voltage [5], (b) predicted output voltage for a triangular section when U = 4.47 m/s and R = 37 kΩ.

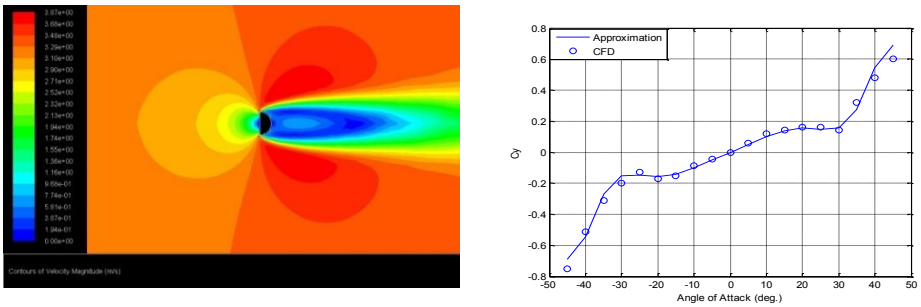

(a) (b)

Fig. 4. (a) Velocity field distribution, (b) steady force coefficient C_y for *D*- section.

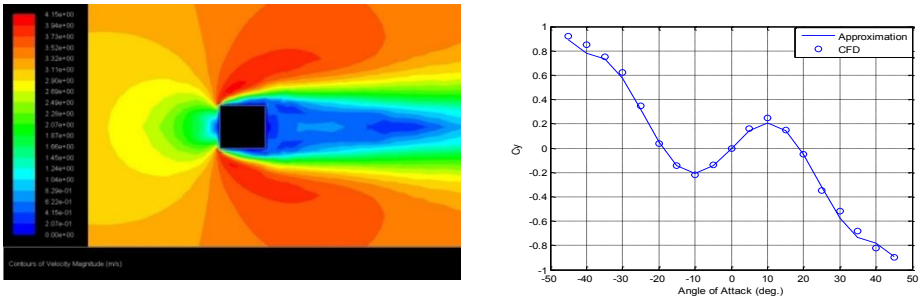

(a) (b)

Fig. 5. (a) Velocity field distribution, (b) steady force coefficient C_y for square section.

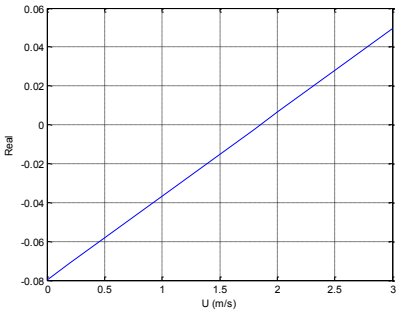

(a)

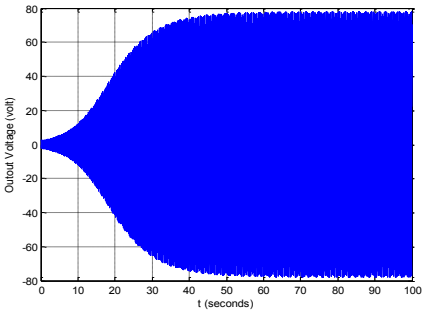

(b)

Fig. 6. (a) Real part of the first eigenvalue, (b) time histories of the harvested voltage when $R = 37$ kΩ and $U = 4.47$ m/s for D-section.

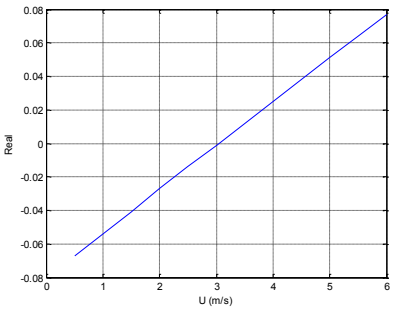

(a)

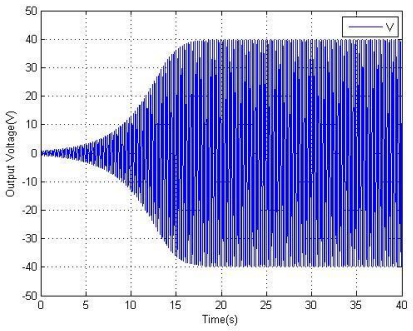

(b)

Fig. 7. (a) Real part of the first eigenvalue, (b) time histories of the harvested voltage when $R = 37$ kΩ and $U = 4.47$ m/s for square section.

4 Conclusions

A piezoelectric energy harvester, based on the concept of aeroelastic galloping was developed in this work. A finite element model was formulated to evaluate the dynamic characteristics of the system. Meanwhile, the lift and drag coefficients of the galloping section are evaluated using CFD. Of the geometries studied, the D- section was found to yield the lowest galloping onset and the greatest galloping behavior and hence the maximum power. Meanwhile, the shortest transient time response was found by the square section of the bluff body. The proposed design is considered to offer a viable solution for a standalone power source for remote wireless sensors.

The authors acknowledge the support of Messrs. Abid Rahman, Rendi Saputro and Yusran Anwar in conducting the Finite Element models and some computations.

References

1. A. Abdelkefi, "Aeroelastic energy harvesting: A review," *International Journal of Engineering Science,* **100**, 112 (2016)
2. S. Anton, R. and H. Sodano, A., "A review of power harvesting using piezoelectric materials (2003–2006)," *Smart Materials and Structures,* **16**, R1 (2007)

3. A. Erturk, W. G. R. Vieira, C. De Marqui, and D. J. Inman, "On the energy harvesting potential of piezoaeroelastic systems," *Applied Physics Letters,* **96**, p. 184103, 2010.
4. S. Roundy and P. K. Wright, "A piezoelectric vibration based generator for wireless electronics," *Smart Materials and Structures,* **13**, 1131 (2004)
5. J. Sirohi and R. Mahadik, "Piezoelectric Wind Energy Harvester for Low-Power Sensors," *Journal of Intelligent Material Systems and Structures,* **16**, 2011 (2011).
6. A. Abdelkefi, A. H. Nayfeh, and M. R. Hajj, "Effects of nonlinear piezoelectric coupling on energy harvesters under direct excitation," *Nonlinear Dynamics,* **67**, 1221 (2012)